2009 fall

Phase Transformation of Materials

12. 08. 2009

Eun Soo Park

Office: 33-316
Telephone: 880-7221
Email: espark@snu.ac.kr
Office hours: by an appointment

1

Contents for previous class

- **Overall Transformation Kinetics – TTT Diagram**

  - Johnson-Mehl-Avrami Equation

  $$f = 1 - \exp(-kt^n)$$

  k : sensitive to temp. (N, v)

  n : 1 ~ 4
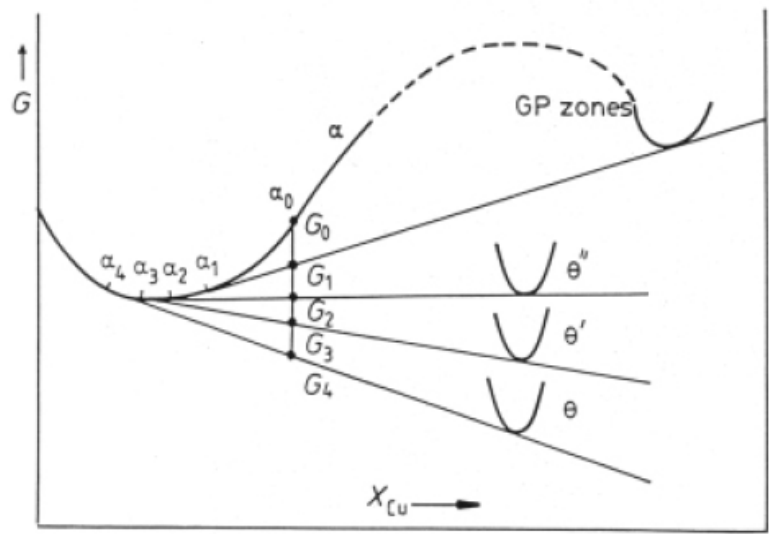
  Growth controlled.   **Nucleation-controlled.**

- **Precipitation in Age-Hardening Alloys**

  $\boxed{\alpha_0}$ **Quenching + Isothermal**

  $\rightarrow \alpha_1 + \text{GP zones}$

  $\rightarrow \alpha_2 + \theta'' \rightarrow \alpha_3 + \theta' \rightarrow \alpha_4 + \theta$

  (**CuAl$_2$**)

- **Quenched-in Vacancies**
  - 불균일 핵생성 위치 제공
  - 원자의 확산속도 증가...핵생성 및 성장속도 증가

- **Age Hardening** : 중간상 형성시 커다란 격자변형 수반하고, 소성 변형시 전위의 이동을 방해함

  최대경도 θ″와 θ′ 공존할때

2

Contents for today's class

- **Spinodal Decomposition**

- **Particle Coarsening (Ostwald Ripening)**

- **Precipitation of Ferrite from Austenite**

- **Eutectoid Transformation**

- **Bainite Transformation**

- **Massive Transformation**

5.5.5 Spinodal Decomposition

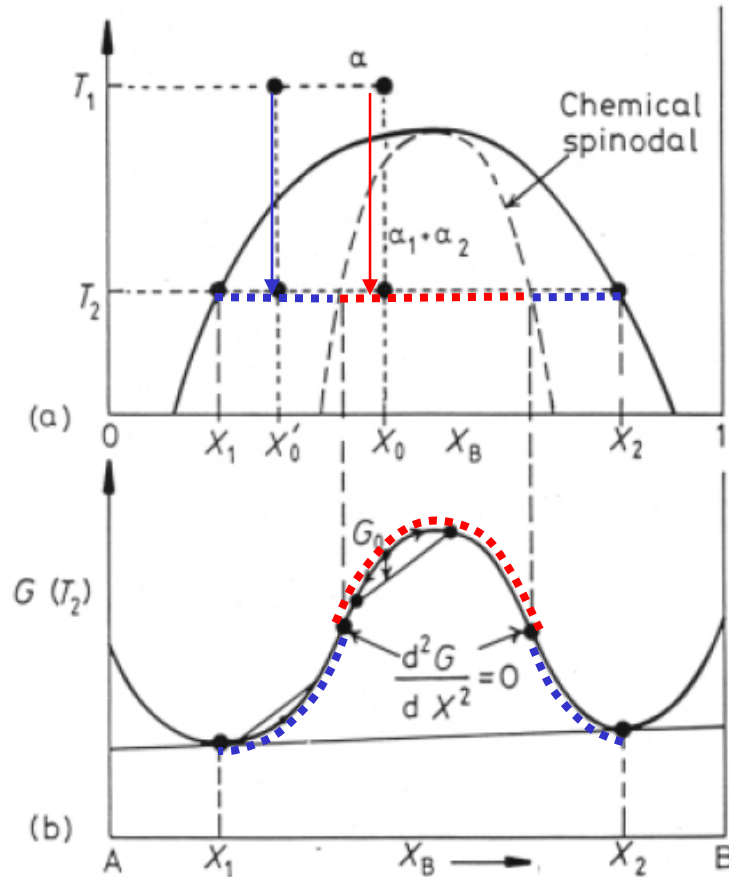## Spinodal mode of transformation has no barrier to nucleation

How does it differ between inside and outside the inflection point of Gibbs free energy curve?

1) Within the spinodal $$\frac{d^2G}{dX^2} < 0$$

: 조성의 작은 요동에 의해 상분리/up-hill diffusion

2) If the alloy lies outside the spinodal, **small variation in composition leads to an increase in free energy and the alloy is therefore metastable.**

The free energy can only be decreased if nuclei are formed with a composition very different from the matrix.

→ nucleation and growth
: **down-hill diffusion**

Fig. 5.38 Alloys between the spinodal points are unstable and can decompose into two coherent phases α_1 and α_2 without overcoming an activation energy barrier. Alloys between the coherent miscibility gaps and the spinodal are metastable and can decompose only after nucleation of the other phase.

4

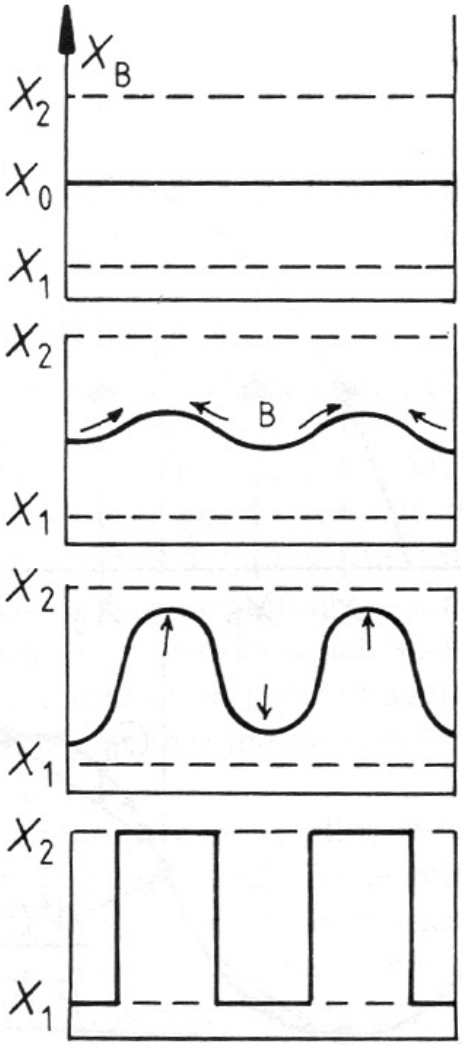# 5.5.5 Spinodal Decomposition

1) Composition fluctuations within the spinodal

2) Normal down-hill diffusion Outside the spinodal

up-hill diffusion
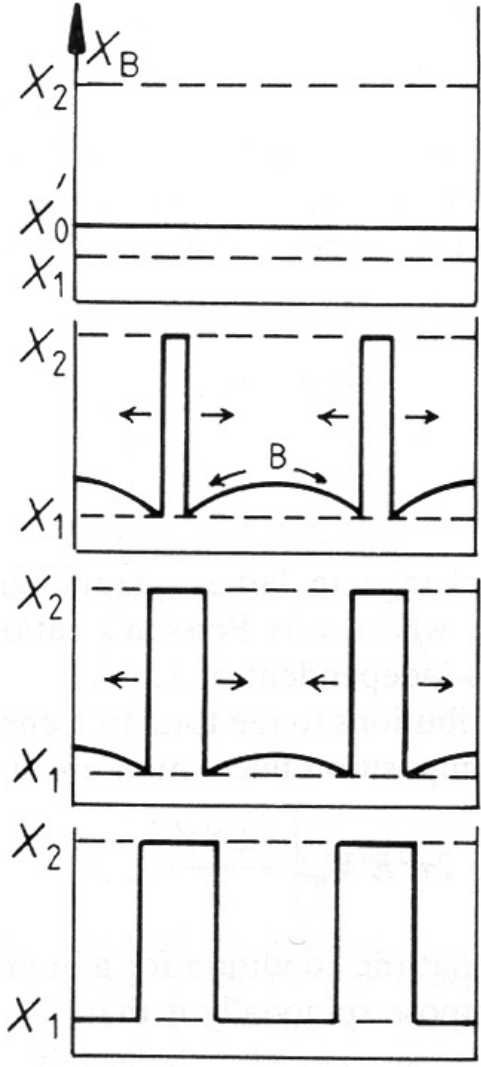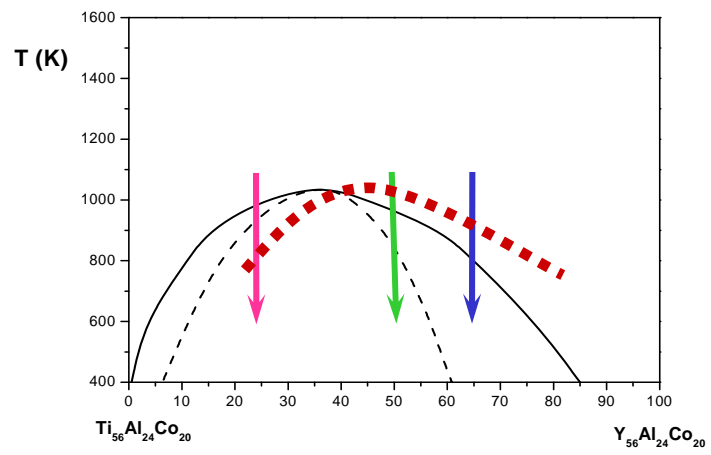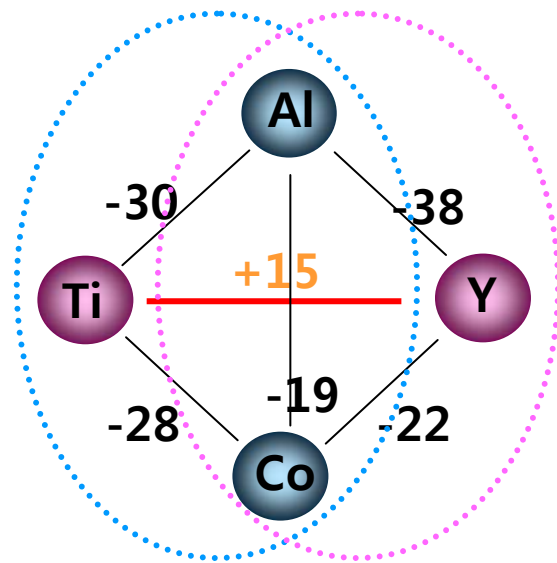
interdiffusion coefficient $D < 0$

down-hill diffusion

Increasing time

Distance

Distance

5

Droplet structure **Interconnected structure** **Droplet structure**

$(Y_{56}Al_{24}Co_{20})_{25}(Ti_{56}Al_{24}Co_{20})_{75}$ $(Y_{56}Al_{24}Co_{20})_{50}(Ti_{56}Al_{24}Co_{20})_{50}$ $(Y_{56}Al_{24}Co_{20})_{65}(Ti_{56}Al_{24}Co_{20})_{35}$
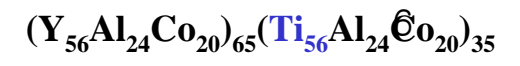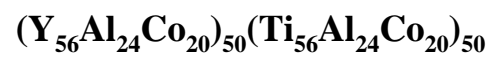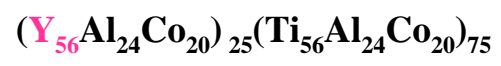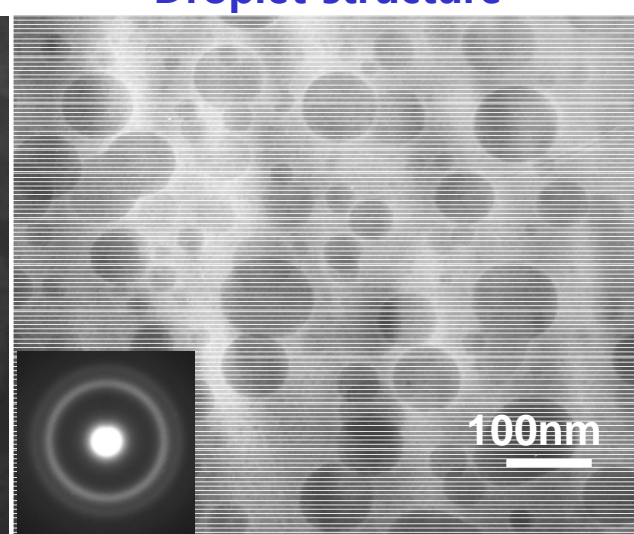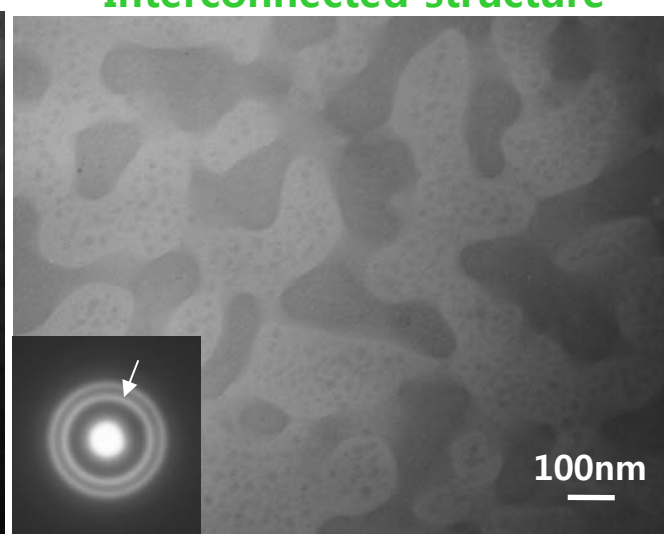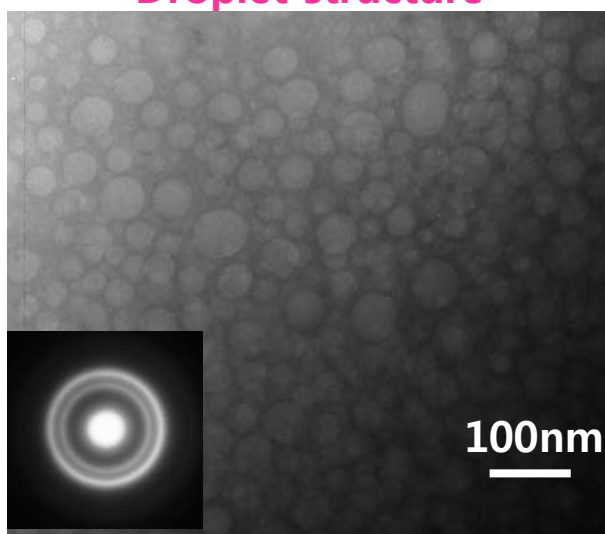
5.5.5 Spinodal Decomposition

* The Rate of Spinodal decomposition

Rate controlled by interdiffusion coefficient D

within the spinodal D<0 & composition fluctuation $\propto \exp(-t/\tau)$

$$\tau = -\lambda^2 / 4\pi^2 D$$

τ: **characteristic time constant**

1차원으로 가정했을 때,
λ: **wavelength of the composition modulations**

$\rightarrow$ Kinetics depends on λ. **Transf. rate ↑ as λ ↓**

최소의 λ 값이 존재하며, 그 값 이하에서는 스피노달 분해가 일어나지 않는다.

5.5.5 Spinodal Decomposition

* Free Energy change for the decomposition

1) Decomposition of X_0 into $X_0 + \Delta X$ and $X_0 - \Delta X$

What would be an additional energy affecting spinodal decomposition?
실제로 일어나는 조성 요동의 파장을 계산하려면,

2) interfacial energy

3) coherency strain energy

1) Decomposition of X_0 into $X_0 + \Delta X$ and $X_0 - \Delta X$

$$\Delta G_{chem} = \frac{1}{2}\frac{d^2 G}{dX^2}(\Delta X)^2$$

$$f(a+h) = f(a) + f'(a)h + \frac{f''(a)}{2!}h^2 + \cdots$$

$$G(X_0 + \Delta X) \approx G(X_0) + G'(X_0)\Delta X + \frac{G''(X_0)}{2!}\Delta X^2$$

$$G(X_0 - \Delta X) \approx G(X_0) - G'(X_0)\Delta X + \frac{G''(X_0)}{2!}\Delta X^2$$

$$\Delta G_{chem} = \frac{G(X_0 + \Delta X) + G(X_0 - \Delta X)}{2} - G(X_0)$$

$$= \frac{G''(X_0)}{2!}\Delta X^2 = \frac{1}{2}\frac{d^2 G}{dX^2}\Delta X^2$$

8

5.5.5 Spinodal Decomposition

2) During the early stages, the interface between A-rich and B-rich region is not sharp but very diffuse. → diffuse interface

Interfacial Energy
(gradient energy)

$$\Delta G_\gamma = K\left(\frac{\Delta X}{\lambda}\right)^2$$

이종 원자사이의 결합수가
증가하기 때문에 생성

K: 동종 혹은 이종 **atomic pair**들의 **bond energy**에 비례하는 비례상수

고용체를 구성하는 원자의 크기가 서로 다르면, 조성차이 ΔX~정합변형 에너지 ΔGs를 유발

3) **Coherency**
   Strain Energy

$$\Delta G_S \propto E\delta^2 \qquad\qquad \delta = (da/dX)\,\Delta X/a$$

(atomic size difference)

δ: misfit, E: Young's modulus, a: lattice parameter

$$\Delta G_S = \eta^2 (\Delta X)^2 E' V_m \qquad where\ \eta = \frac{1}{a}\left(\frac{da}{dX}\right), E' = E/(1-\nu)$$

ΔGs는 λ에 무관

η: **fractional change in lattice parameter per unit composition change**

• 조성의 요동으로 생긴
  전체 자유 E의 변화
  1) + 2) + 3)

$$\Delta G = \left\{\frac{d^2 G}{dX^2} + \frac{2K}{\lambda^2} + 2\eta^2 E' V_m\right\}\frac{(\Delta X)^2}{2}$$

5.5.5 Spinodal Decomposition

$$\Delta G = \left\{ \boxed{\frac{d^2G}{dX^2} + \frac{2K}{\lambda^2} + 2\eta^2 E' V_m} \right\} \frac{(\Delta X)^2}{2}$$
$$< 0$$

* Condition for Spinodal Decomposition

균질한 고용체가 불안정하게 되어
스피노달 분해를 할 수 있는 조건

$$-\frac{d^2G}{dX^2} > \frac{2K}{\lambda^2} + 2\eta^2 E' V_m$$

* The Limit for the decomposition
스피노달 분해가 가능한 온도와 조성의 한계값

$$\lambda \to \infty$$

$$\frac{d^2G}{dX^2} = -2\eta^2 E' V_m$$

→ coherent spinodal **(next page)**

Wavelength for coherent spinodal

$$\lambda^2 > -2K \bigg/ \left(\frac{d^2G}{dX^2} + 2\eta^2 E' V_m \right)$$

→ The minimum possible wavelength decreases with increasing undercooling below the coherent spinodal.

10

5.5.5 Spinodal Decomposition

Coherent Miscibility Gap

This is the line defining the equilibrium compositions of the coherent phases that result from spinodal decomposition.
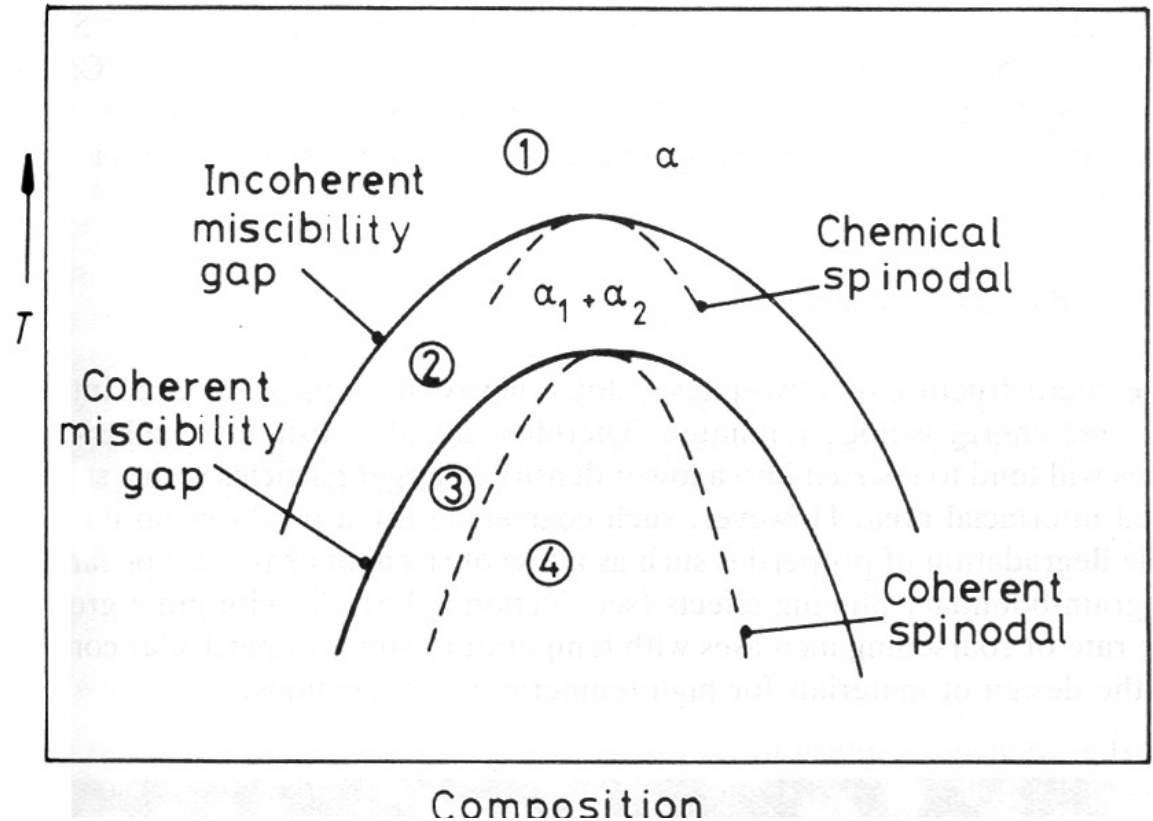
- ΔT between the coh. and incoh. Miscibility gap, or the chemical and coh.

Spinodal : dependent of $|\eta|$

- Large atomic size diff. $\rightarrow$ $|\eta|$ large 변형에너지 효과를 극복하기 위해서는 매우 큰 과냉도 필요

5.5.6. Particle Coarsening

Two Adjacent Spherical Precipitates with Different Diameters

(Gibbs-Thomson effect)
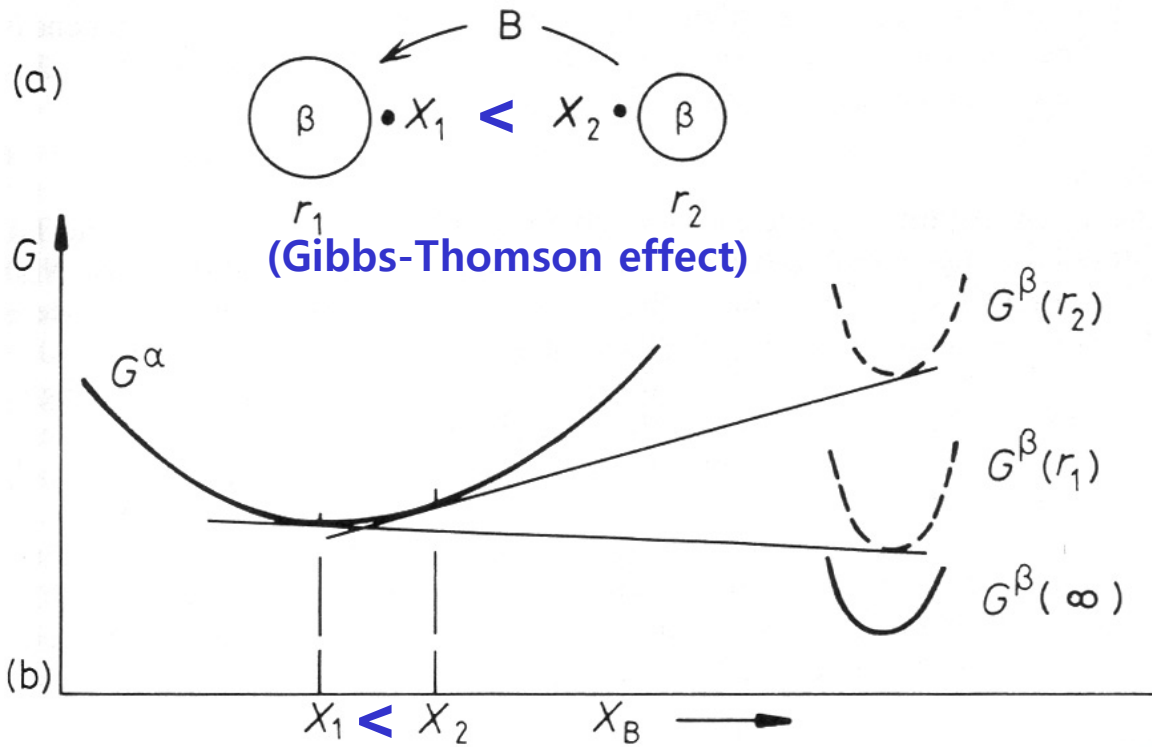
체적확산이 속도 제어 인자라면,

$$(\bar{r})^3 - r_0^3 = kt$$

where $k \propto D\gamma X_e$

(X_e: 매우 큰 입자와의 평형용해도)

$$\frac{d\bar{r}}{dt} \propto \frac{k}{\bar{r}^2}$$

$\left[\dfrac{D \text{ and } X_e \sim \exp(-Q/RT)}{\bar{r}}\right]$

12
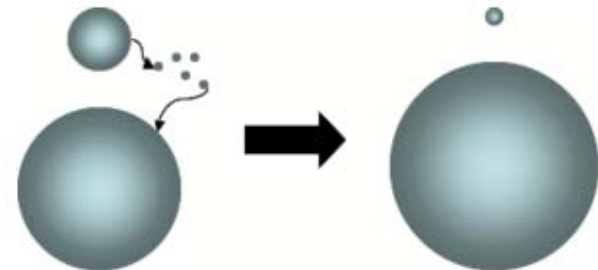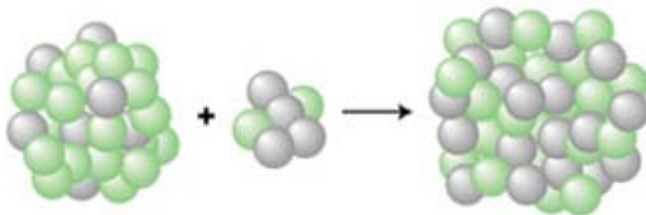
(Ostwald Ripening)

5.5.6. Particle Coarsening

**The Rate of Coarsening
with Increasing Time and Temp.**
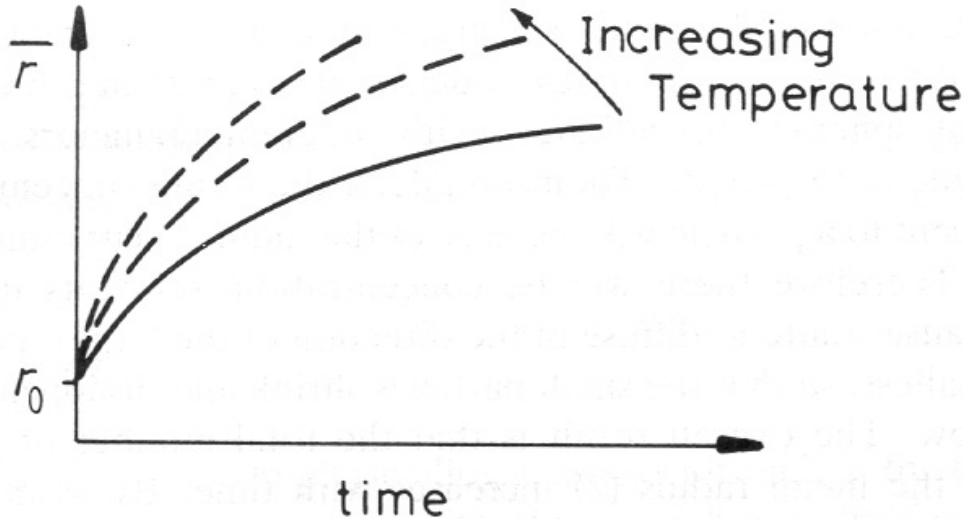
r_0 : mean radius at time t=0

$\overline{r}$ ~ 고온재료의 기계적 특성과 밀접한 관계
조대화가 일어나면 강도 감소 및 기계적 성질이 저하됨.

**How can you design an alloy
with high strength at high T?**

hint) $\dfrac{d\overline{r}}{dt} \propto \dfrac{k}{\overline{r}^2}$ $k \propto D\gamma X_e$

1) low γ

**heat-resistant Nimonic alloys
based on Ni-Cr**

→ **ordered fcc $Ni_3(Ti,Al)$ (=γ')**

Ni/γ'의 계면 완전 정합관계 **(10 ~ 30 mJ m^{-2})**

고온에서도 미세한 조직 유지 가능
→ **creep 특성 향상**

2) low X_e

fine oxide dispersion (분산강화)
ThO_2 (thoria) for W and Ni

금속에서 산화물의 낮은 용해도에 기인

3) low D

Cementite → high D of carbon

매우 빠르게 조대화

**a. substitutional alloying element
segregated in the carbide**

**b. strong carbide-forming elements
(also low X_e)**

13

5.6. The Precipitation of Ferrite from Austenite

(Grain boundary and the surface of inclusions)

The Iron-Carbon Phase Diagram
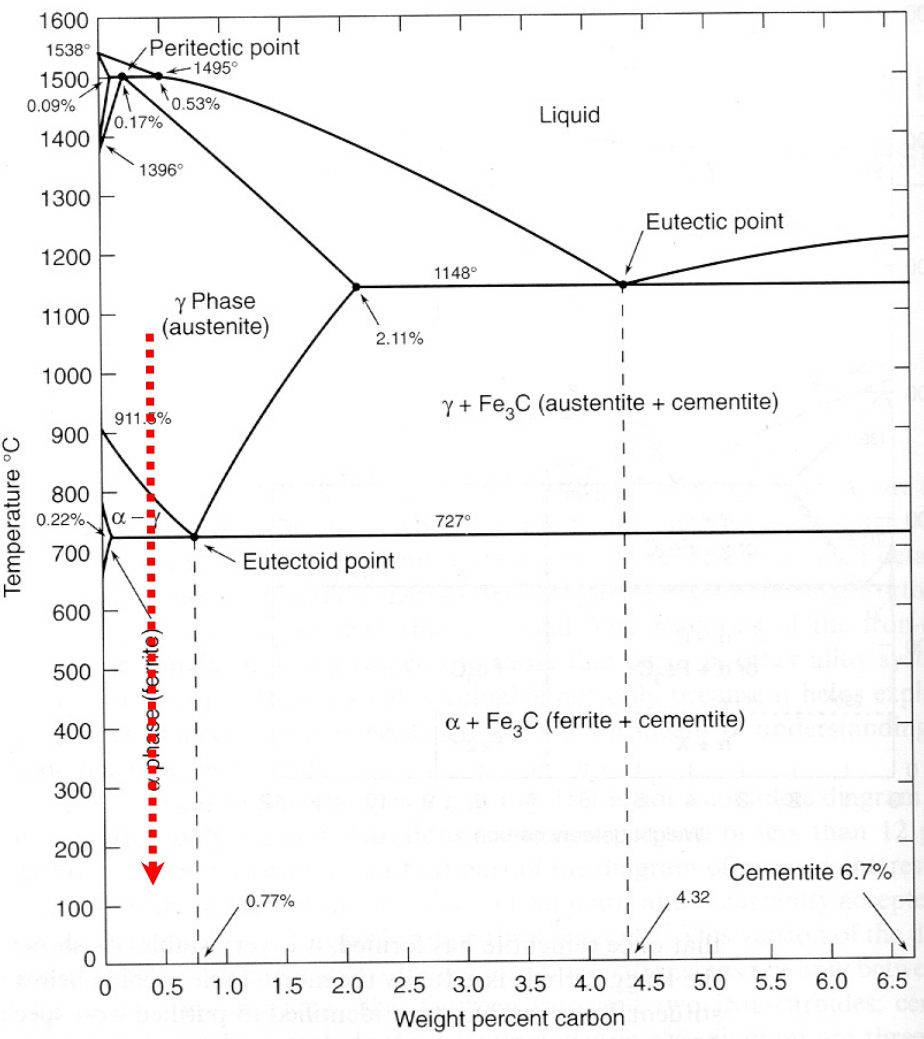
Microstructure (0.4%C) evolved by slow cooling (air, furnace) ?
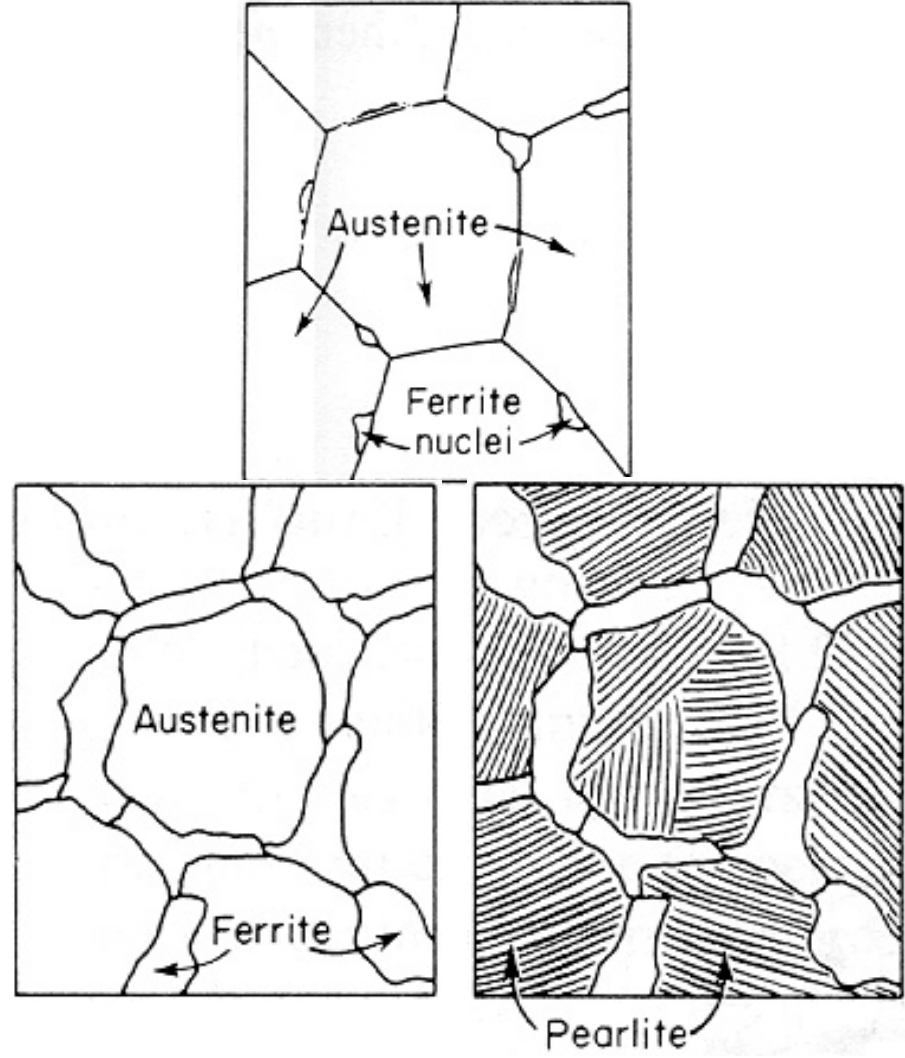
5.6. The Precipitation of Ferrite from Austenite

Diffusional Transformation of Austenite into Ferrite
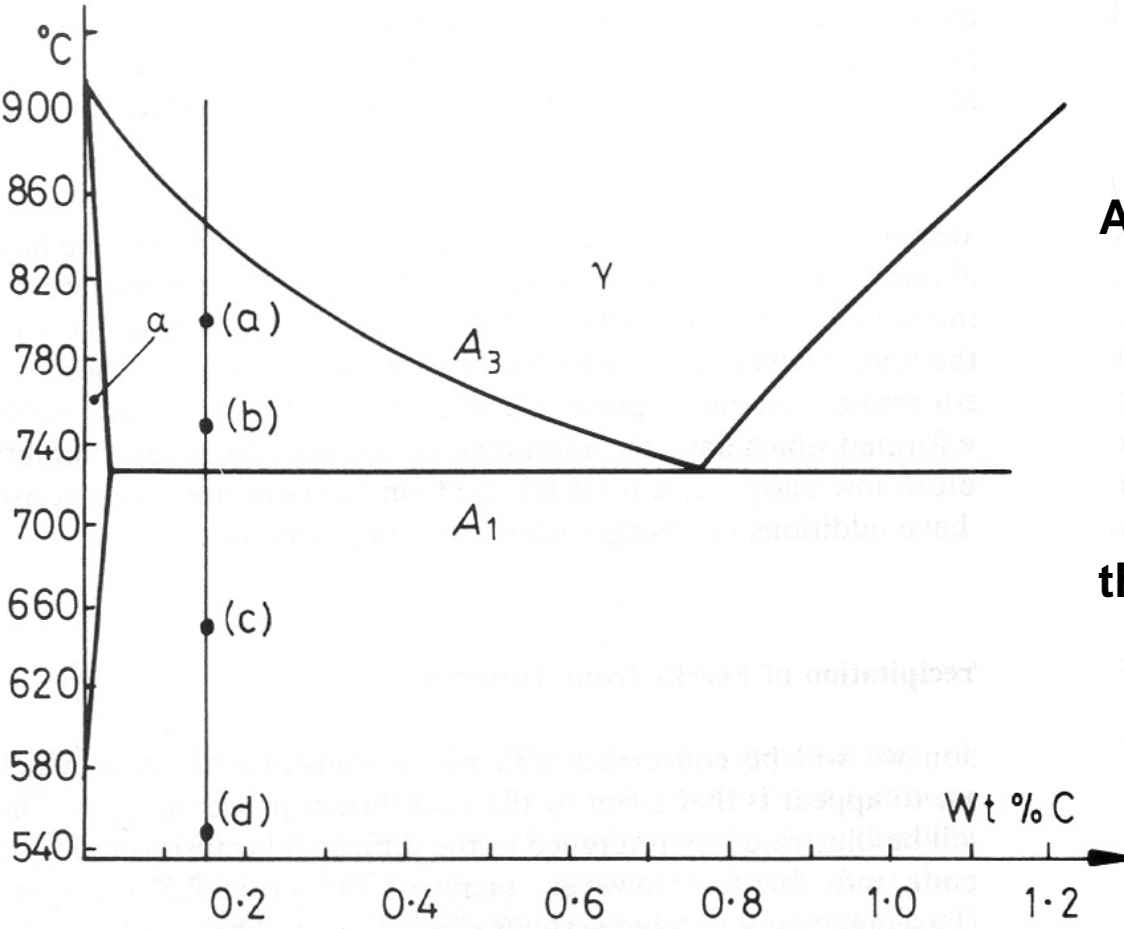
Fe-0.15%C

After being austenitized, held at
(a) 800°C for 150 s
(b) 750°C for 40 s
(c) 650°C for 9 s
(d) 550°C for 2 s and
then quenched to room T.

What would be the microstructures?

5.6. The Precipitation of Ferrite from Austenite

Microstructures of an Fe-0.15%C alloy austenitized

초석 Ferrite가 판상으로 성장

판상 Ferrite 수 증가/주로 입계로부터 성장

(a) 800ºC for 150 s

(c) 650ºC for 9 s

입계타형
GB allotriomorphs

(b) 750ºC for 40 s

(d) 550ºC for 2 s
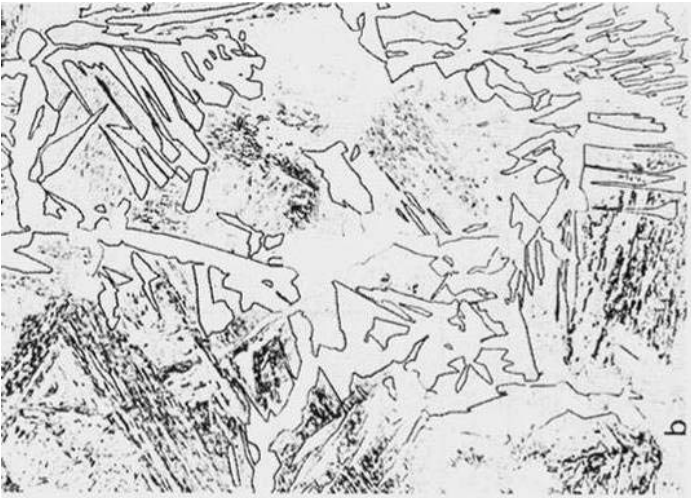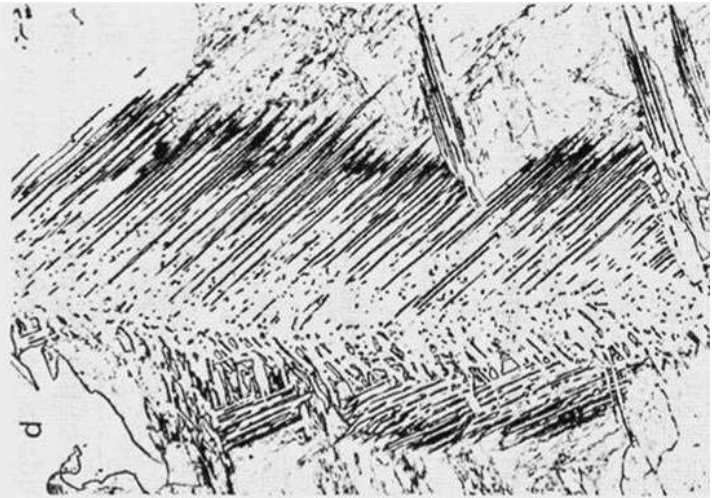
White area γ → α, Gray area: γ → M **Widmanstätten side plates (b), (c), (d)**

과냉도가 클수록 더 미세하게 됨

5.6. The Precipitation of Ferrite from Austenite

Relative Velocity of Incoherent & Semicoherent Interfaces

At small undercoolings, **it is proposed that both semi-coherent and incoherent interfaces can migrate at similar rates, while at large undercoolings only incoherent interfaces can make full use of the increased driving force.**
(Continuous growth)

과냉도가 클수록
더 미세하게 됨

Allotriomorphos

거의 Equiaxed 형상
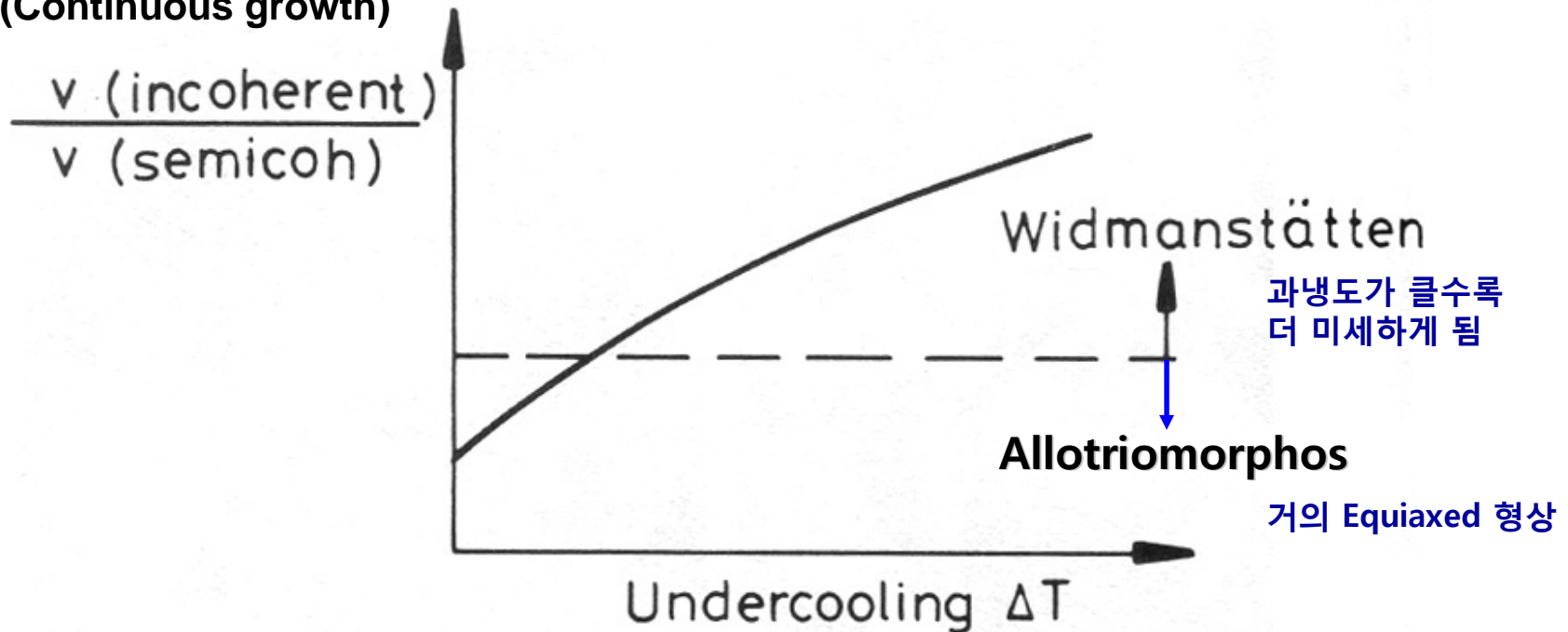
The reason for the transition from grain boundary allotriomorphs to Widman-stätten side-plates with increasing undercooling is not fully understood.

Intragranular ferrite: ferrite can also precipitate within the austenite grains
inclusions and dislocations/ large-grained specimen

5.6. The Precipitation of Ferrite from Austenite

Typical TTT curve for $\gamma \rightarrow \alpha$ transformation

$$\rightarrow \quad f(\text{t,T})$$

J-M-A Eq. $\quad f = 1 - \exp(-kt^{n})$
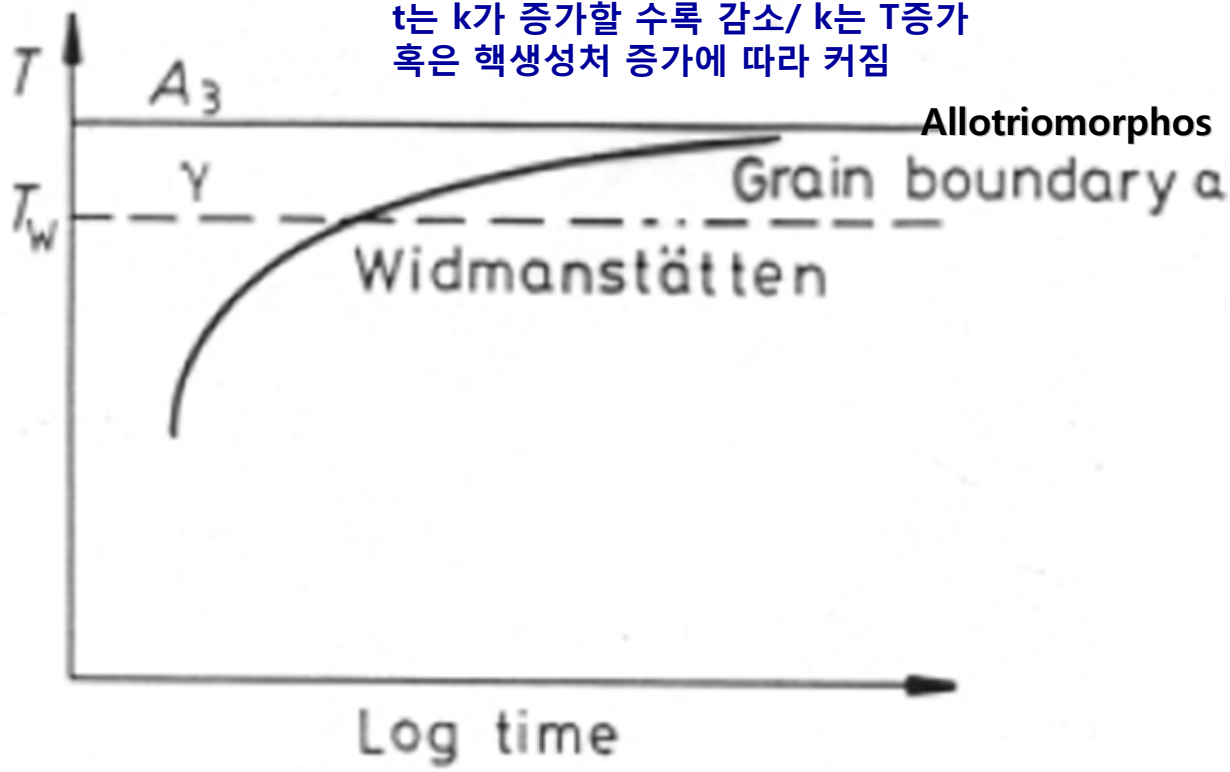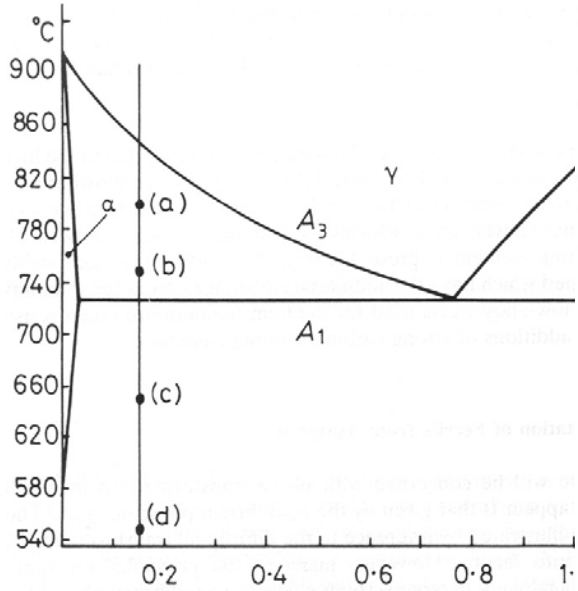
t는 k가 증가할 수록 감소/ k는 T증가
혹은 핵생성처 증가에 따라 커짐

A TTT diagram for the precipitation of ferrite
in a hypoeutectoid steel will have **a typical C shape.**

18

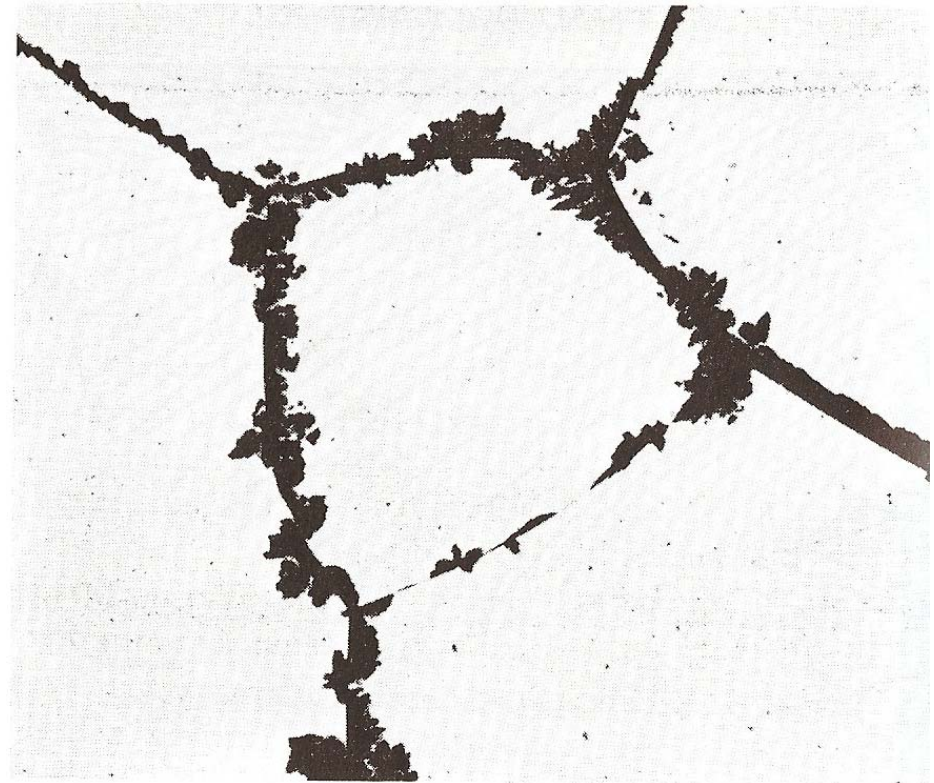# 5.6. The Precipitation of Ferrite or Fe$_3$C from Austenite

(b)
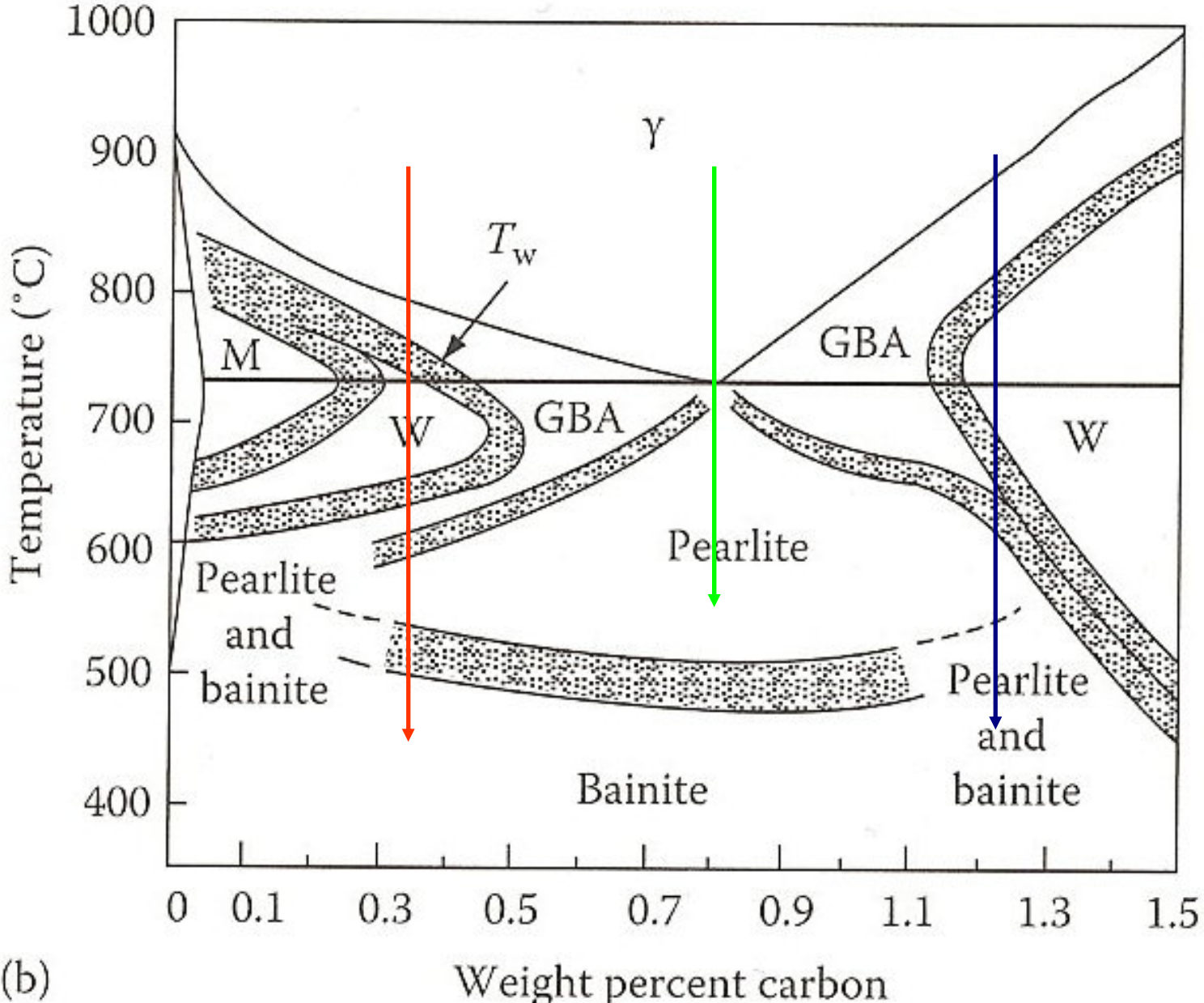
Eutectoid Transformation

Pearlite Reaction in Fe-C Alloys

$$\gamma \;\rightarrow\; \alpha \;\; + \;\; Fe_3C$$
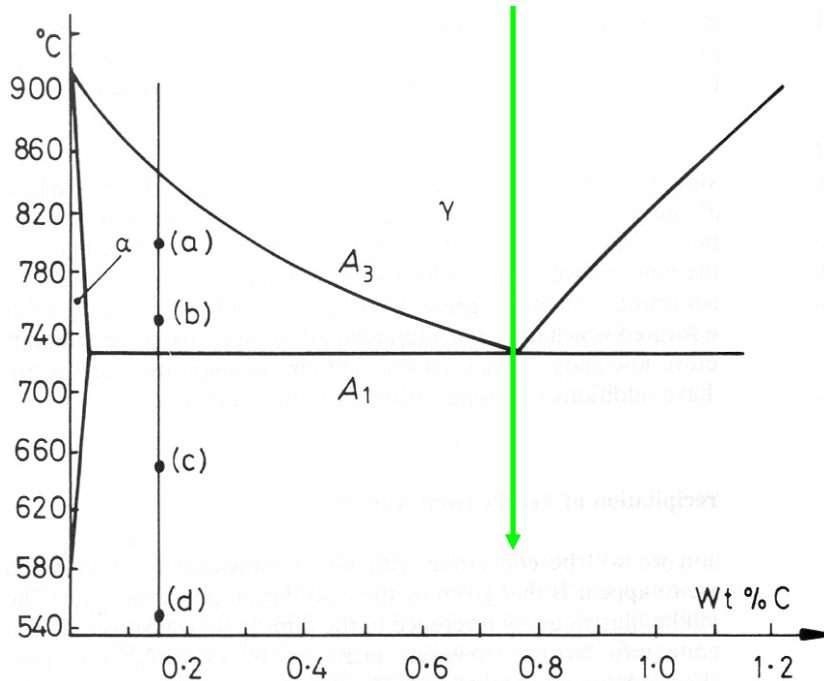
Pearlite nodule 은 입계에서 핵을 생성하며
거의 일정한 속도로 입자안으로 성장한다.

* A1 이하로 과냉도가 작은 경우,
 : 생성된 펄라이트 노듈의 수가 비교적 적고 서로 방해받지 않고 반구나 구형태로 성장
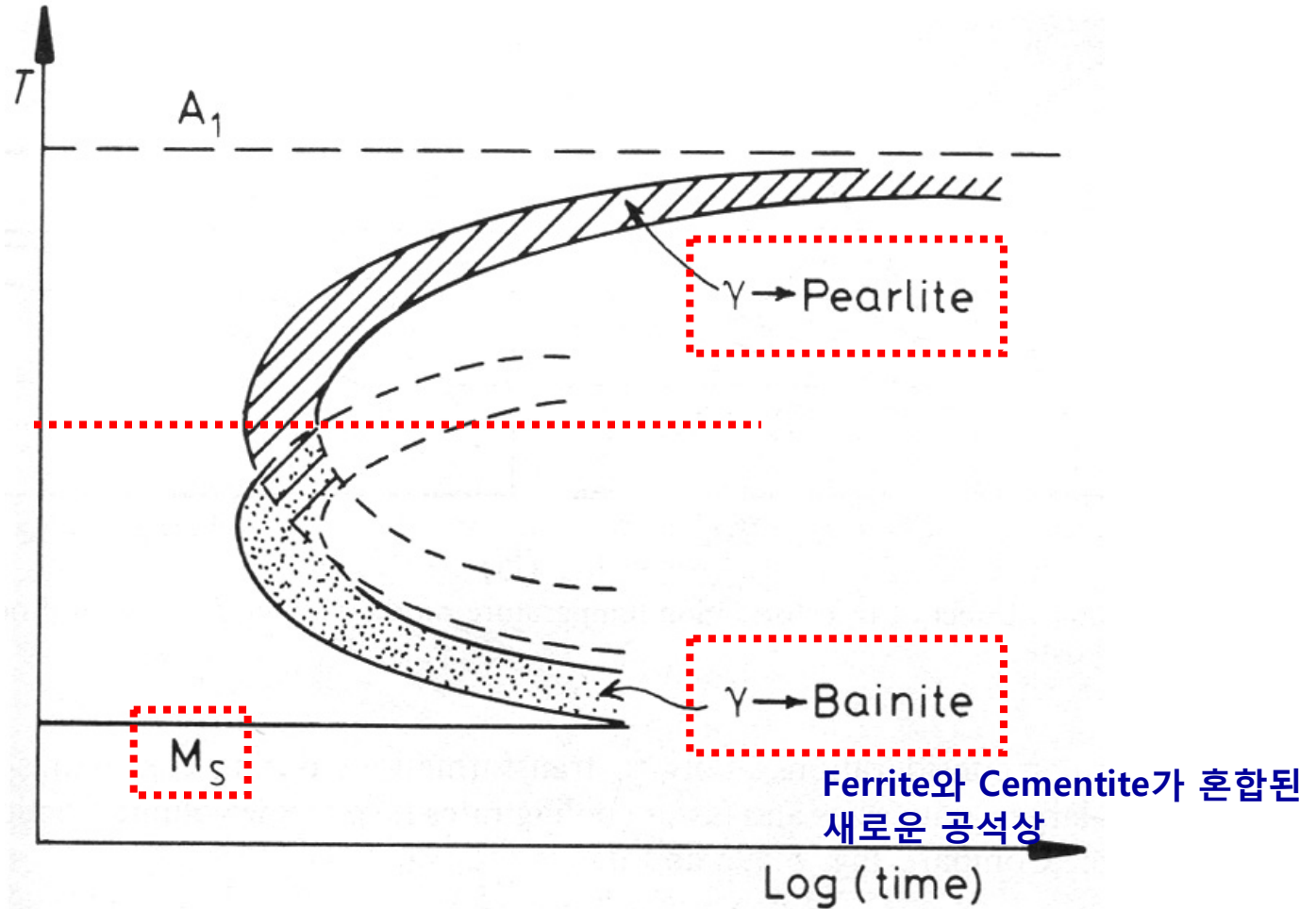* 과냉도가 큰 경우,
 : 핵생성 속도가 커서 가능한 모든 위치에 핵생성 일어나 모든 입계가 펄라이트 모듈로 덮힘.

Pearlite Reaction in Fe-C Alloys
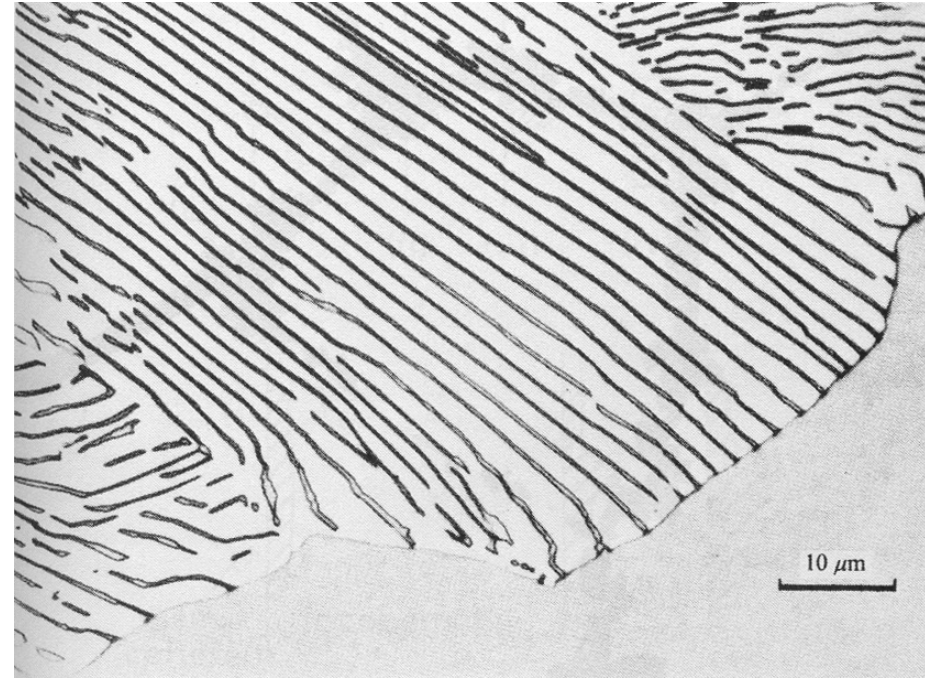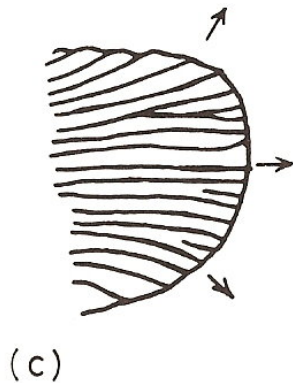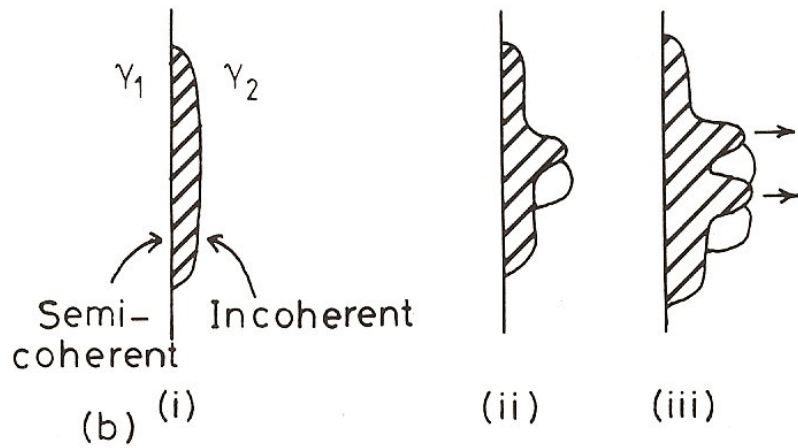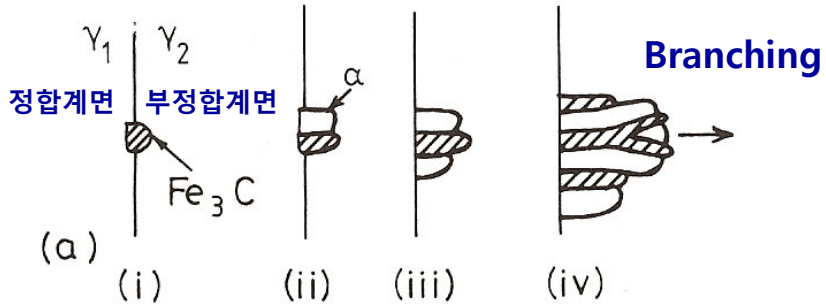
Pearlite grows into the austenite grain with which it does not have an orientation relationship.

Growth of Pearlite

**Relative Positions of the Transformation curves
for Pearlite and Bainite in Plain Carbon Eutectoid Steels.**

Ferrite와 Cementite가 혼합된
새로운 공석상

Bainite Transformation

미세구조는 Bainite가 생성되는 온도에 따라 달라짐

Upper Banite in medium-carbon steel

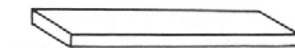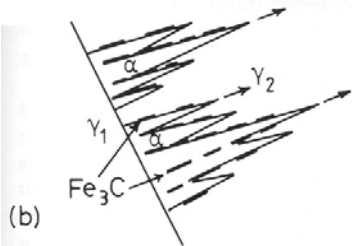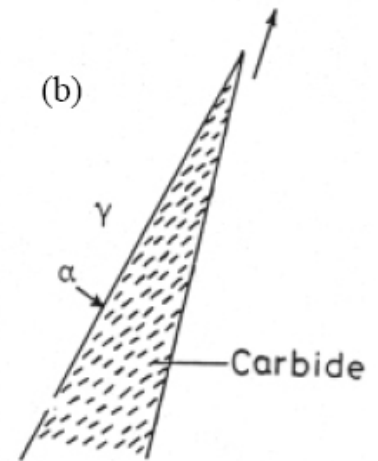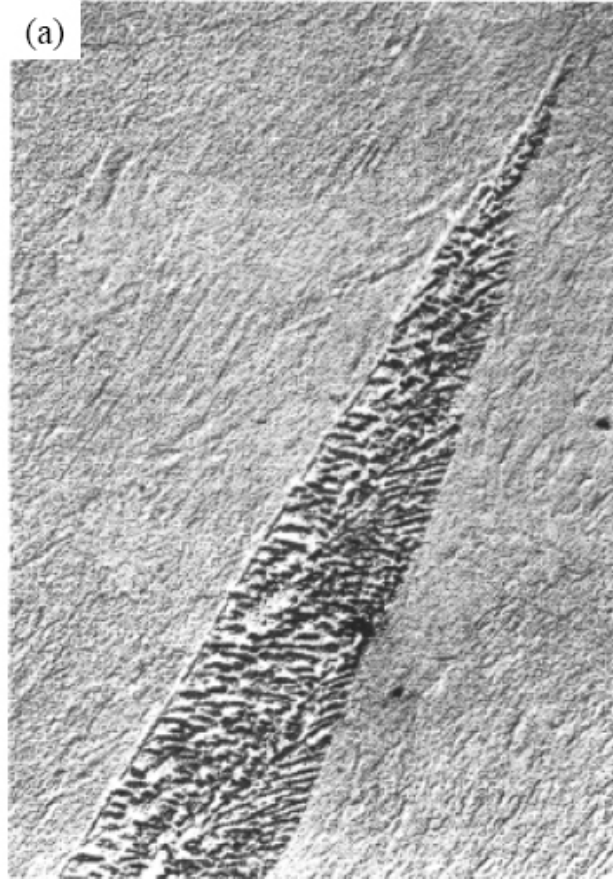**350 ~ 550°C, laths, K-S relationship, similar to Widmanstäten plates**

침상이나 래스 형태의 Ferrite와 사이에서 석출된 Fe_3C
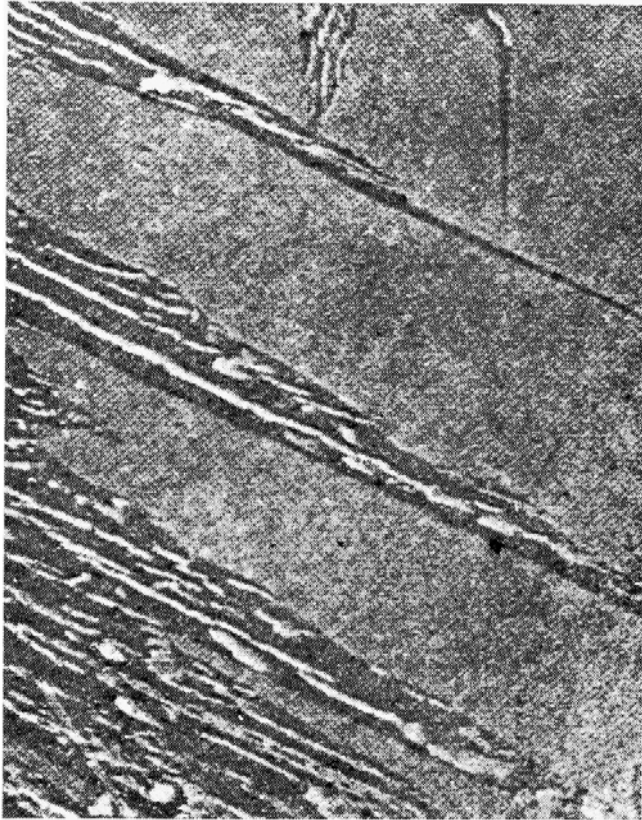
Lower Bainite in 0.69wt% C low-alloy steel

조직: 래스모양 →판상
탄화물 매우 미세하게 분산, M에서와 유사

Martensite
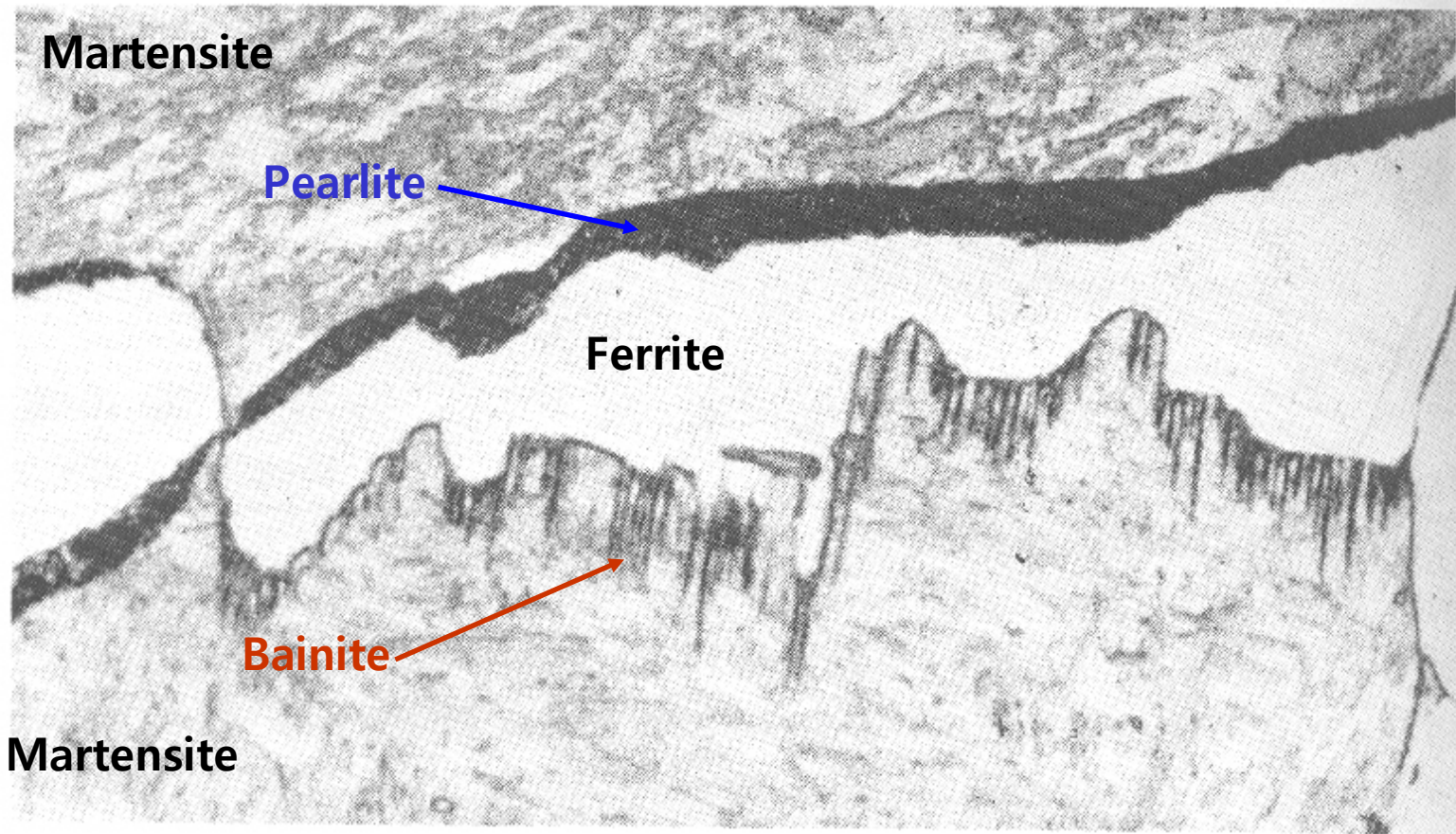
Pearlite

Ferrite

Bainite

Martensite

Fig. 5.62 Hypoeutectoid steel (0.6% C) partially transformed for 30 min at 710 °C, inefficiently quenched. Bainitic growth into lower grain of austenite and pearlitic growth into upper grain during quench (× 1800). (After M. Hillert in *Decomposition of Austenite by Diffusional Processes*, V.F. Zackay and H.I. Aaronson (Eds.), 1962, by permission of the Metallurgical Society of AIME.)

Pearlite : no specific orientation relationship
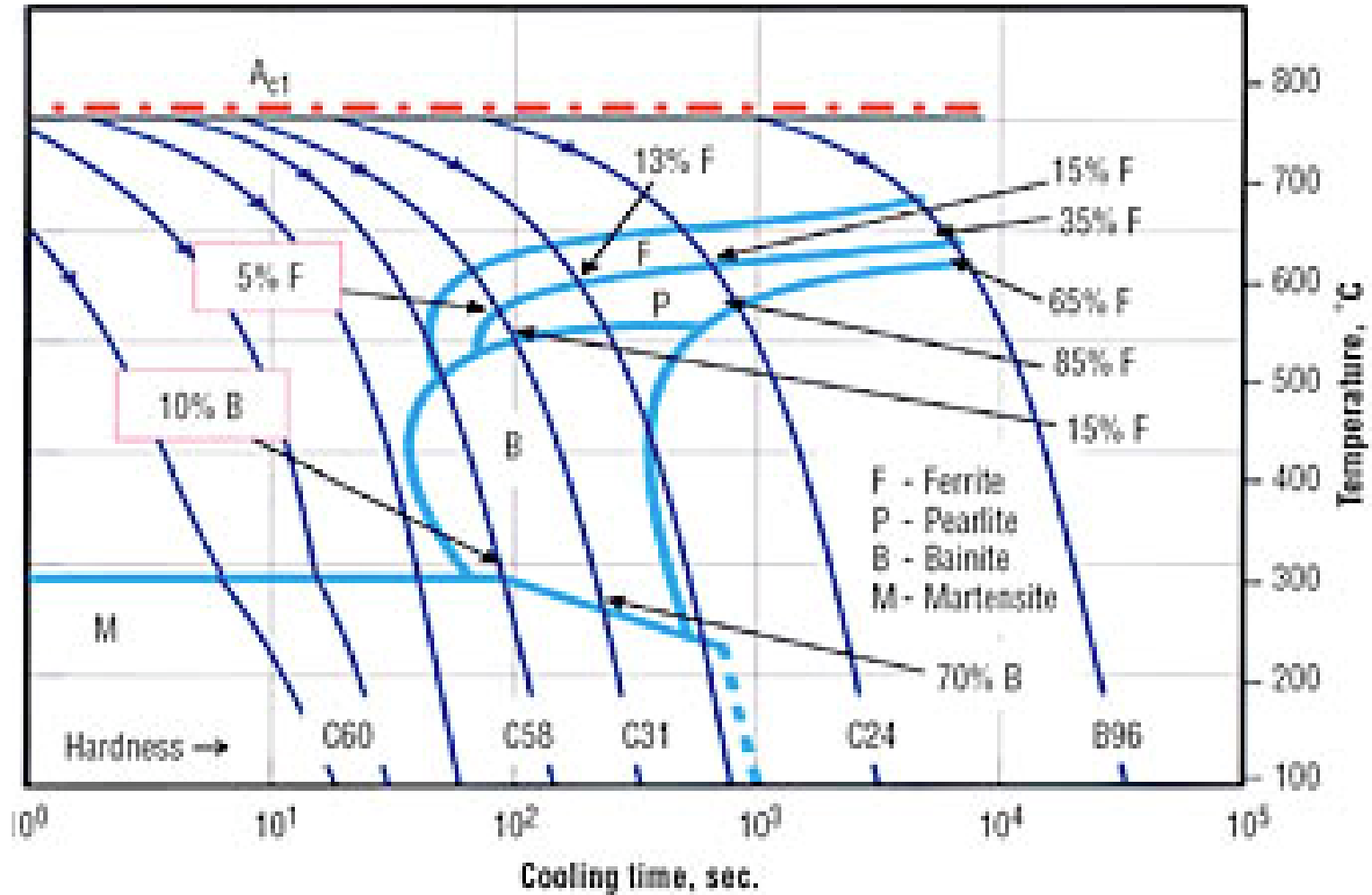
Bainite : orientation relationship

24

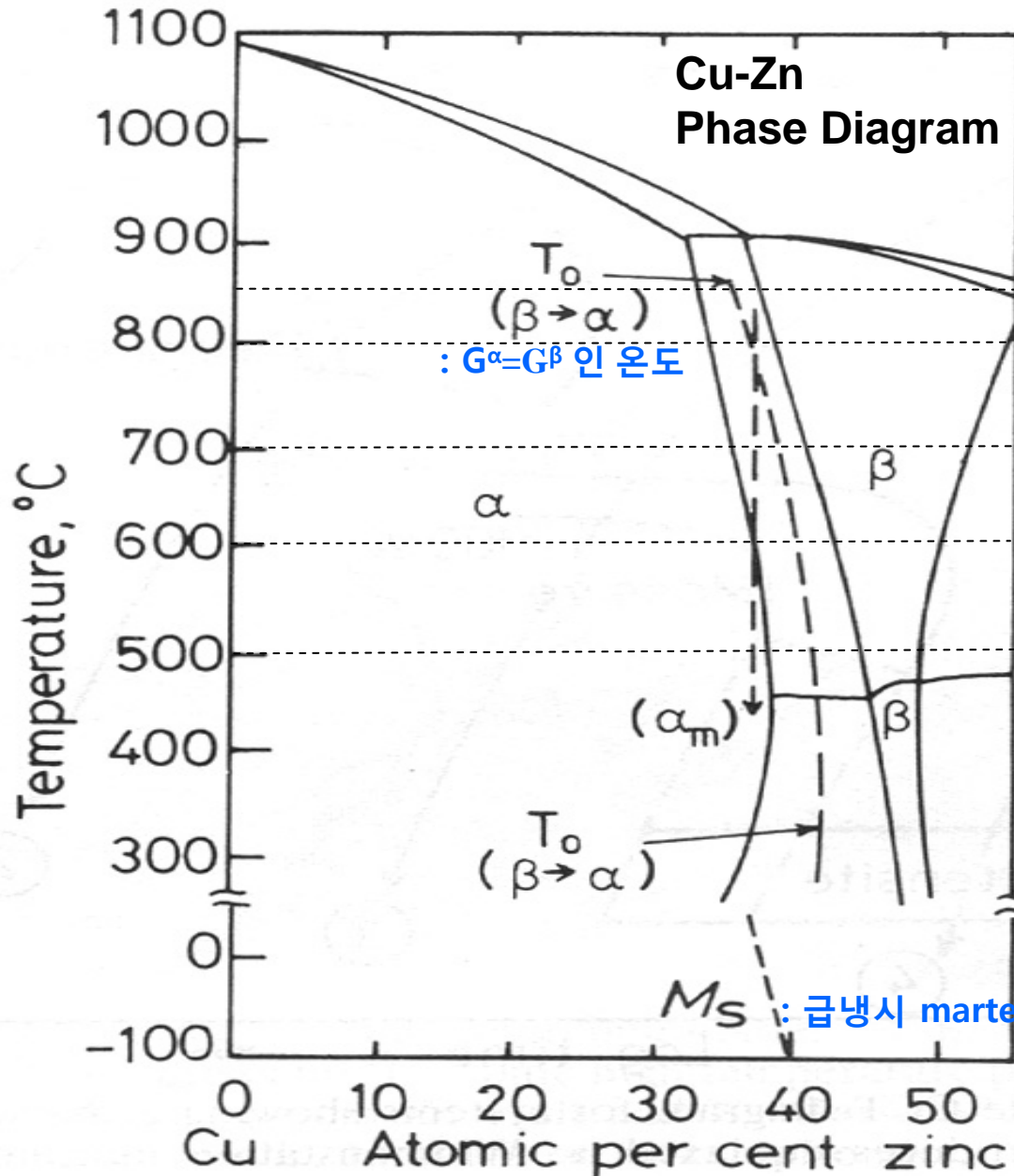# 5.8.4. Continuous Cooling Transformation diagrams

TTT diagrams
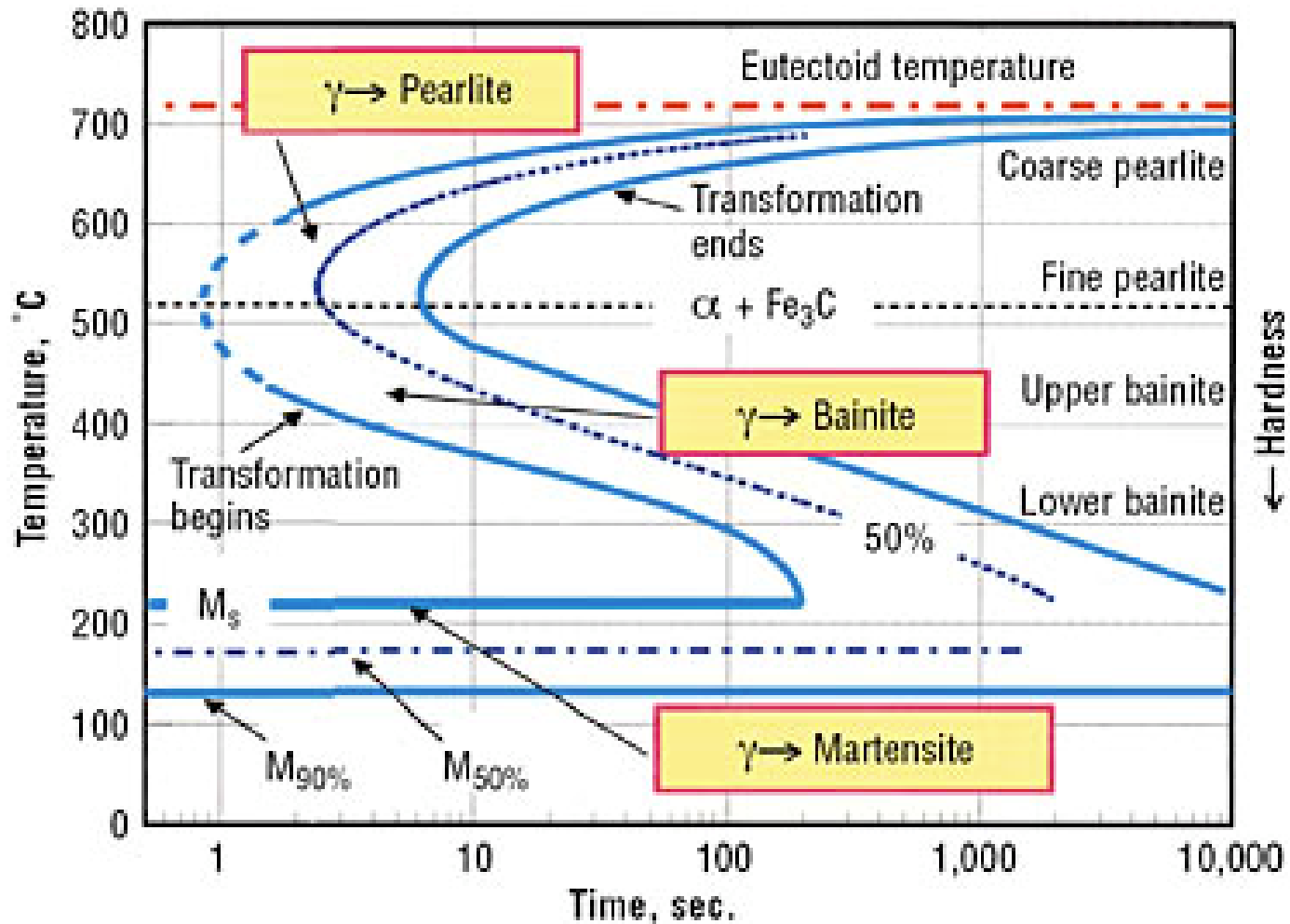
5.8.4. Continuous Cooling Transformation diagrams

CCT diagrams

Massive Transformation

: 조성 변화 없이 결정구조가
다른 단상 또는 다상으로 분해

Cu-Zn Phase Diagram

Free energy-composition curves for α and β at 850°C, 800°C, 700°C and 600°C?

T_o ($\beta \rightarrow \alpha$)

: $G^\alpha = G^\beta$ 인 온도

β

α

(α_m)

β

T_o ($\beta \rightarrow \alpha$)

M_S : 급냉시 martensite 변태 시작 온도

Temperature, °C

Cu   Atomic per cent zinc

27

Massive Transformation

Massive 변태: 급냉후 600 ℃ 이하에서 β 상 유지, 이 온도에서 β→α 로 빠르게 변태
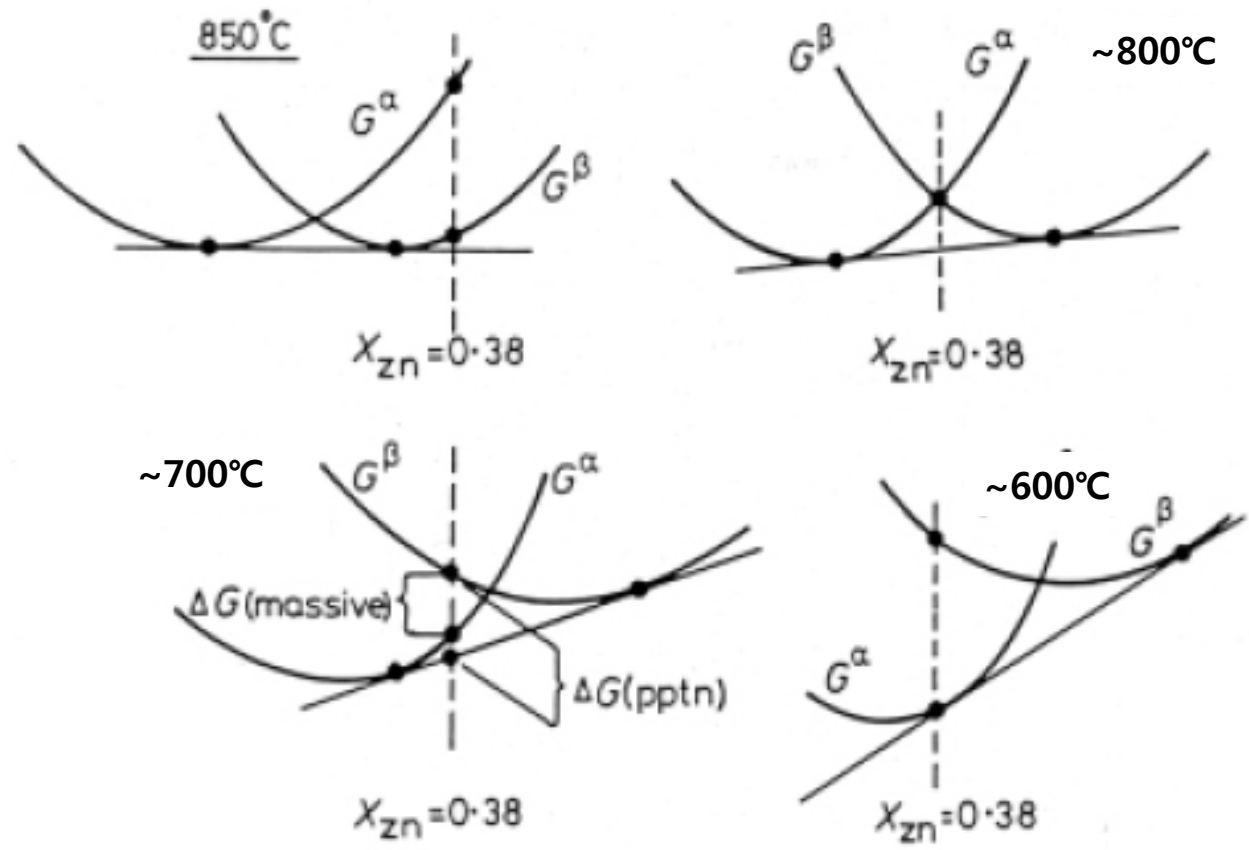
Free energy-composition curves for α and β

Fig. 5.77 A schematic representation of the free energy-composition curves for α and β in the Cu-Zn system at various temperatures.

: 열역학적인 관점에서 볼 때 매시브 변태는 평형상태도의 T_0 온도 이하의 2상 영역내에서도 일어날 수 있지만, 실제로 매시브 변태는 보통 평형상태도의 단상구역에서만 일어난다는 실험적 증거가 많이 보고됨.
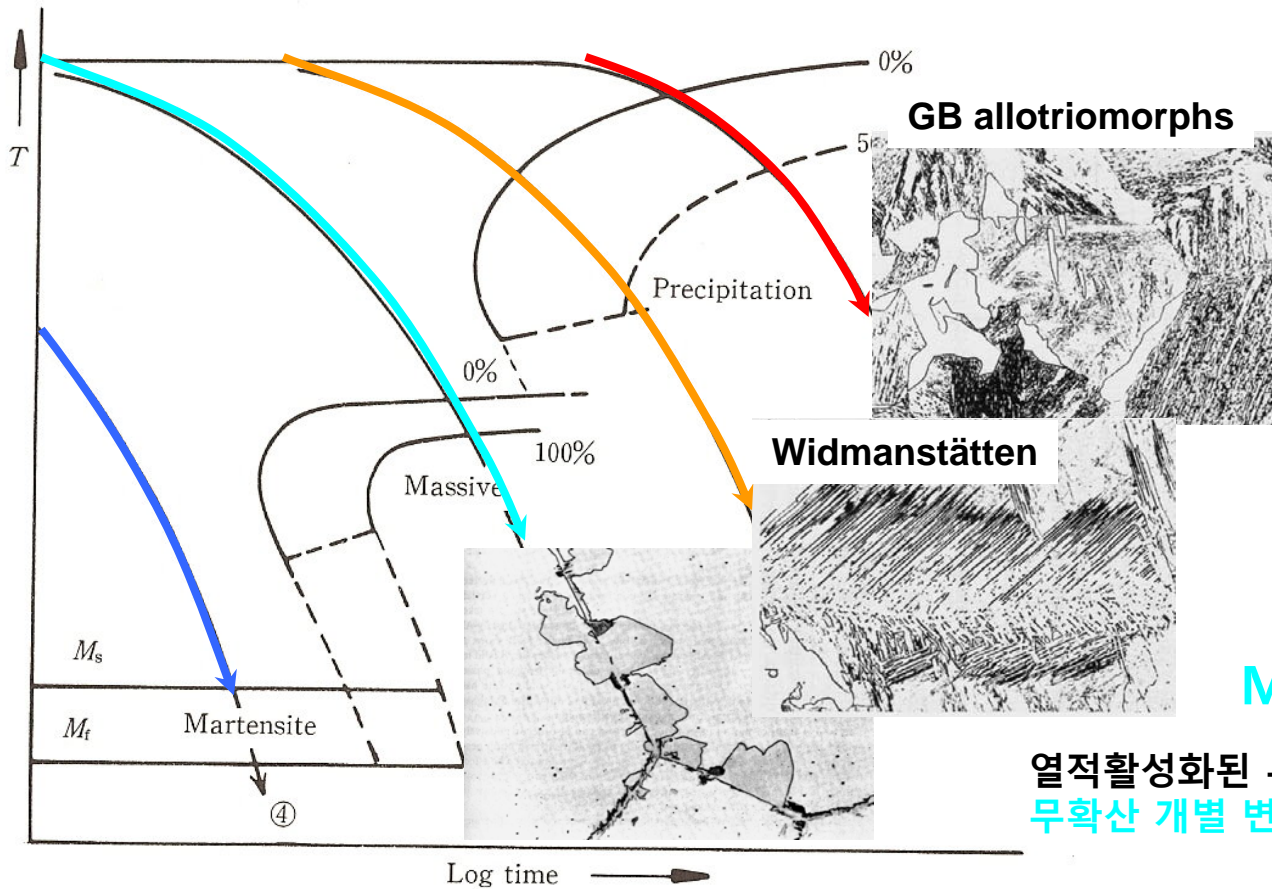
Massive Transformation

Massive α formed at the GBs of β and grow rapidly into the surrounding β.

: 장범위 확산이 아니라 Cu와 Zn 원자들이 α/β 계면 가로지르는 속도로 성장 (∵α 조성 = β 조성)
성장속도가 빠르기 때문에 α/β 계면은 불규칙한 모양을 가짐.

• Massive, Martensite Transformation

GB allotriomorphs

Widmanstätten

T, Ms, Mf, Martensite, Precipitation, Massive, 0%, 100%, ④, Log time

Massive Transformation

열적활성화된 부정합계면의 이동에 의한 성장:
무확산 개별 변태 (diffusionless civilian trans.)

β상의 원자들이 협동적인 이동에 의해 평활 이동 계면을 통과하여 a상으로 전단 변형
무확산 집단 변태
(diffusionless military trans.)

Martensite Transformation

그림 5.75   매시브 변태가 일어나는 합금계에서의 여러 가능한 연속냉각 변태곡선 으로 그림 5.79를 참조하여 볼 것 ① : 서냉시 등축정 α가 생성됨. ② 냉각속도가 증가하면 Widmanstätten 형상의 조직이 생성됨. ③ 냉각속도가 더욱 증가하면 매시 브 변태가 일어남. ④ 가장 빠른 냉각속도에서는 마르텐사이트 변태가 일어남.
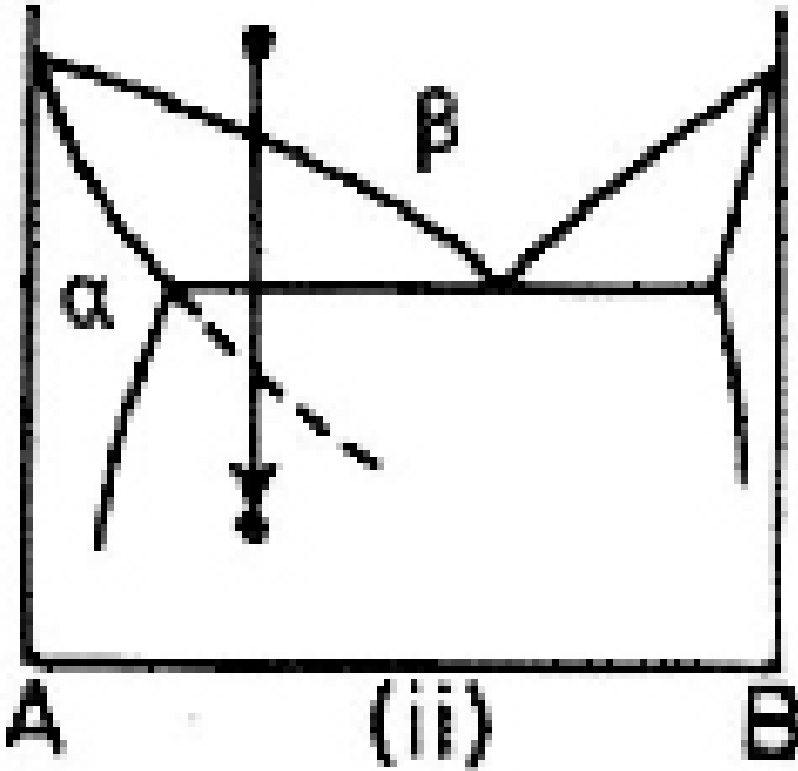
30

Massive Transformation

Effect of Cooling Rate on the Transformation Temperature of Pure Iron
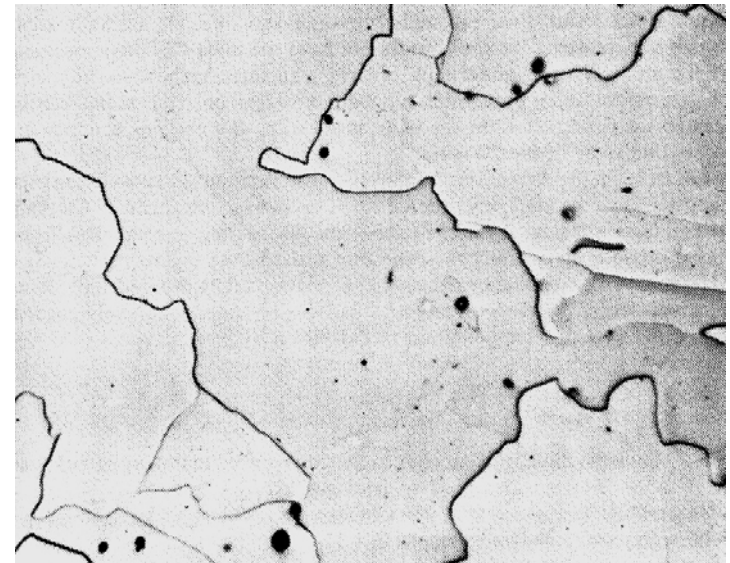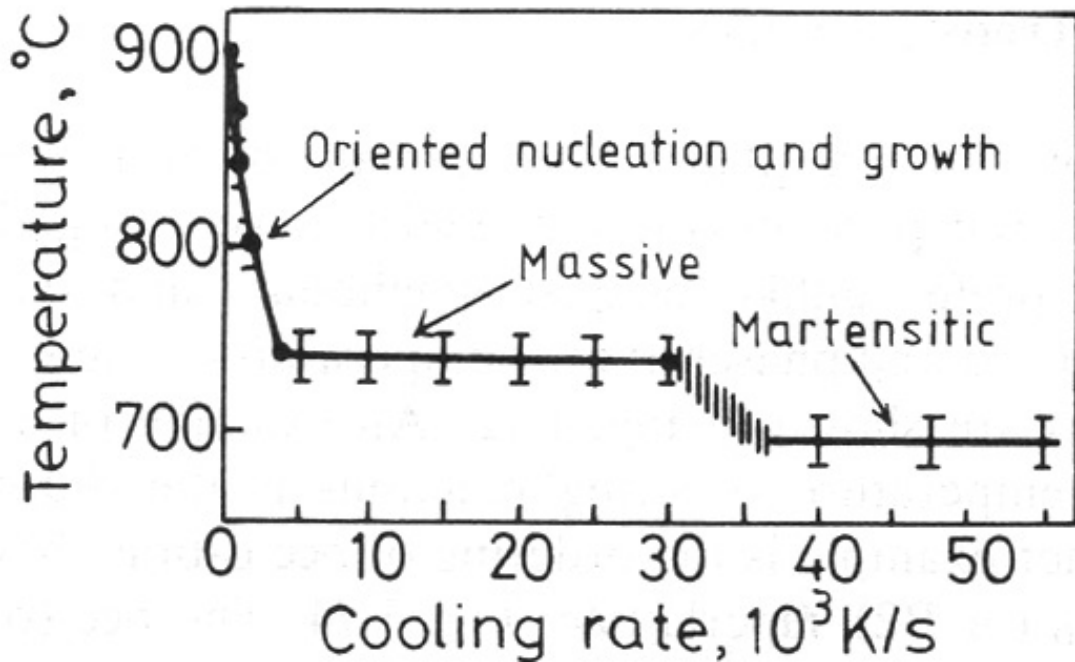
Massive α in an Fe-0.002wt%C
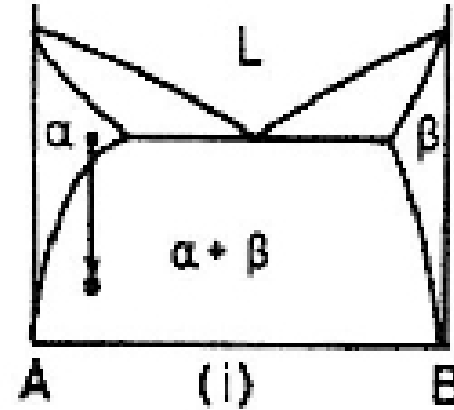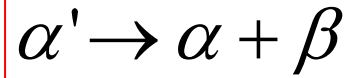
: 불규칙한 α/α 입계가 생성됨.

Massive Transformation

Metastable phases can also form massively.

It is not even necessary for the transformation product to be a single phase: two phases, at least one of which must be metastable, can form simultaneously provided they have the same composition as the parent phase.

5. Diffusion Transformations in solid

(a) Precipitation

$$\alpha' \rightarrow \alpha + \beta$$

Homogeneous Nucleation

$$\Delta G = -V\Delta G_V + A\gamma + V\Delta G_S$$

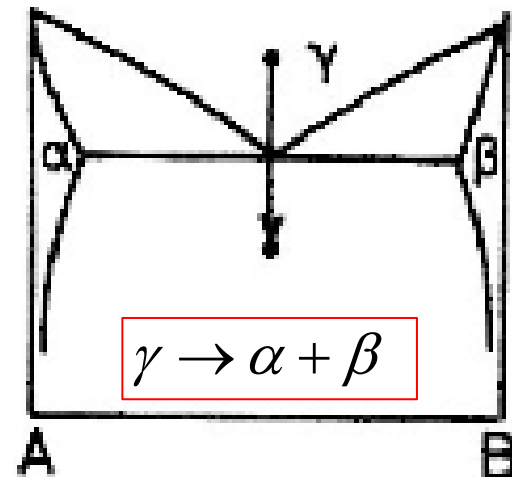$$N_{hom} = \omega\, C_0 \exp\left(-\frac{\Delta G_m}{kT}\right) \exp\left(-\frac{\Delta G^*}{kT}\right)$$

Heterogeneous Nucleation

$$\Delta G_{het} = -V(\Delta G_V - \Delta G_S) + A\gamma - \Delta G_d$$

➡ **적합한 위치는 격자결함
(핵생성이 격자결함 제거 역할)**

(b) Eutectoid Transformation

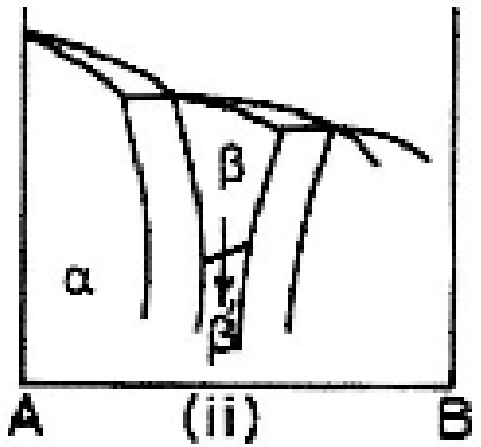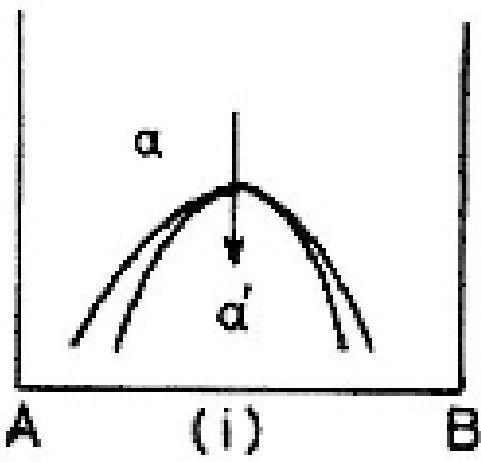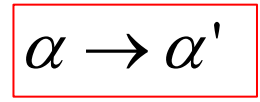**Composition of product phases
differs from that of a parent phase.**
→ **long-range diffusion**
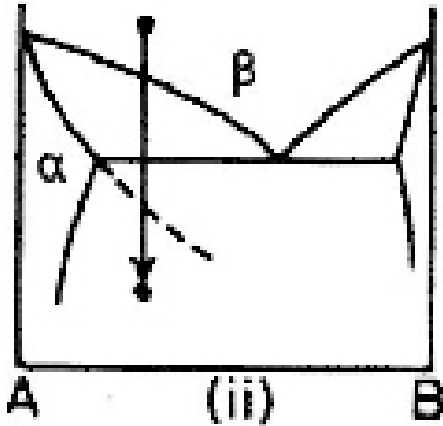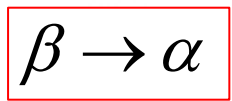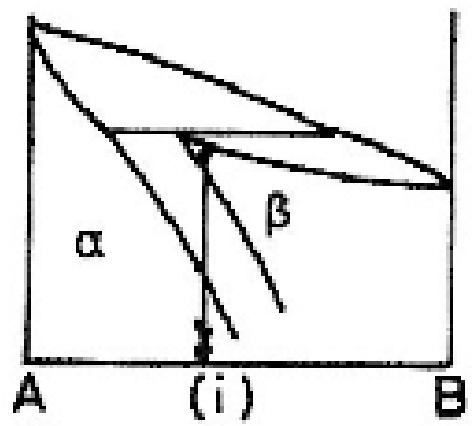
**Which transformation proceeds
by short-range diffusion?**

$$\gamma \rightarrow \alpha + \beta$$

3

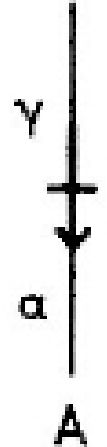# 5. Diffusion Transformations in solid

(c) Order-Disorder Transformation

$$\alpha \rightarrow \alpha'$$

(d) Massive Transformation

: 조성 변화 없이 결정구조가 다른 단상 또는 다상으로 분해

$$\beta \rightarrow \alpha$$

(e) Polymorphic Transformation

: 온도 범위에 따라 서로다른 결정구조가 안정